IEICE TRANS. COMMUN., VOL. E77-B, NO. 10 OCTOBER 1994

PAPER

An Analysis of the Rotational Symmetry of the Inner Field of Radial Line Slot Antennas

Masaharu TAKAHASHI†, Makoto ANDO†† *and* Naohisa GOTO††, *Members*

SUMMARY A radial line slot antenna (RLSA) is a slotted waveguide planar array for the direct broadcast from satellite (DBS) subscriber antennas. A single-layered RLSA (SL-RLSA) is excited by a radially outward traveling wave. The antenna efficiency of more than 85% has already been realized. These antennas are designed on the assumption of perfectly rotationally symmetrical traveling wave excitation; the slot design is based upon the analysis of a slot pair on the rectangular waveguide model with periodic boundary walls. However, the slots perturb the inner field and the actual antenna operation is not perfectly symmetrical. This causes the efficiency reduction especially for very small size antenna. This paper presents a fundamental analysis of the inner field of the radial waveguide. It is impossible to analyze all the slot pairs in the aperture as it is and only the slots in the inner few turns are considered since these provide dominant perturbation. The calculated results are verified by the experiments and reasonable agreement is demonstrated. Some design policies are suggested for enhancing the rotational symmetry.

key word: *RLSA, radial waveguide, planar antenna, method of moment, rotational symmetry, inner field*

1. Introduction

A radial line slot antenna (RLSA) is a slotted waveguide planar array for the direct broadcast from satellite (DBS) subscriber antennas [1],[2]. A single-layered RLSA (SL-RLSA) is attractive in term of structural simplicity as well. It utilizes spirally arrayed slots with non-uniform length which cancels the tapered aperture illumination associated with a radially outward traveling wave excitation [3],[4]. The antenna efficiency of more than 85% has been realized. Some of these antennas are now released for commercial use [5].

These antennas are designed on the assumption of rotationally symmetrical traveling wave excitation. The slot design is conducted by using the rectangular waveguide model which reflects symmetry [6]. However, this analysis model does not perfectly explain the operation of RLSAs. Figure 1 shows the example of experimental aperture field distribution measured above the slot plate, which reflects the inner field in the oversized radial line. The change in amplitude along ϕ-direction is no less than 5dB. This figure indicates the rotational symmetry of the inner field is considerably perturbed due to the spiral slot arrangement [7]. This causes the antenna efficiency reduction, which becomes notable in smaller antenna where larger slot coupling is adopted. In the latest design of RLSA, the matching element [8],[9] is adopted at the periphery of the aperture to perfectly reduce the termination loss power. The rotationally symmetrical traveling wave operation is highly desired for the utilization of these ultimate elements. The conventional waveguide model with periodic wall gives us no information about the symmetry at all.

This paper presents a fundamental analysis of the inner field of the radial line slot antenna. Inner field perturbation due to spiral arrangement of slots is analyzed. In terms of computational capability, it is impossible to analyze all the slot pairs in the aperture as they are. The coupling of the slots in the first few turns of the spiral in the central aperture are analyzed by the method of moment, since they seems to disturb the inner field seriously. The effects of the slot length and the spacings between slot pairs are mentioned. The calculated results are verified by the experiments and fine agreement is demonstrated. To enhance the rotational symmetry, some design policies in spiral arrangement are presented. As an ideal design, annularly arrayed slot pairs excited by a rotating mode is proposed.

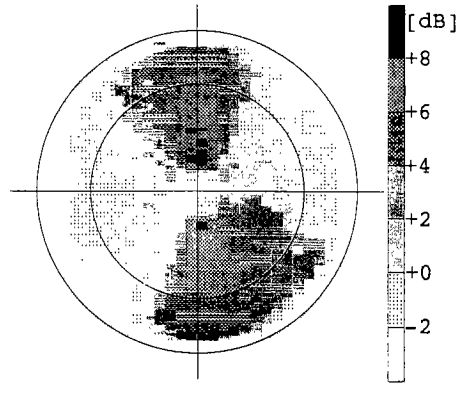

Fig. 1 Aperture amplitude distribution along ϕ-direction on RLSA
Diameter=0.6 m.

Manuscript received March 30, 1994.
Manuscript revised May 23, 1994.

† The author is with the Faculty of Engineering, Musashi Institute of Technology, Tokyo, 158 Japan.
†† The authors are with the Faculty of Engineering, Tokyo Institute of Technology, Tokyo, 152 Japan.

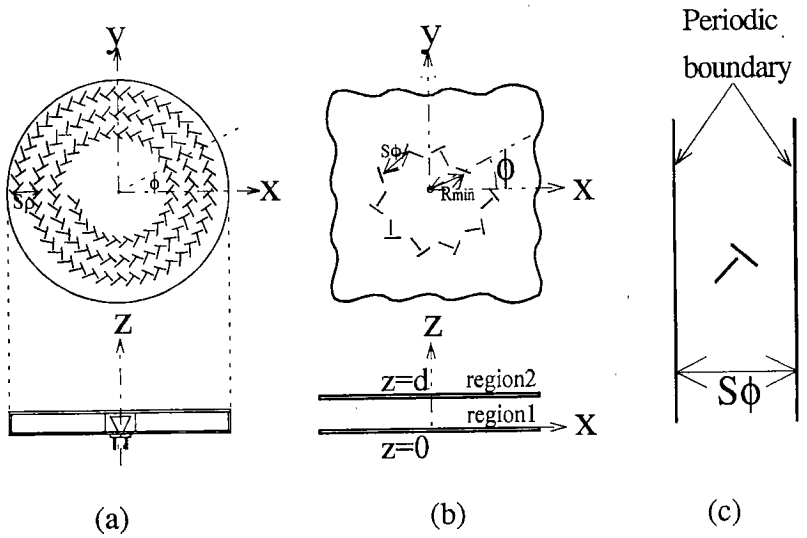

Fig. 2 Analysis model.
(a) SL-RLSA.
(b) Analysis model.
(c) Waveguide model.

2. Analysis

2. 1 Analysis Model

Figure 2(a) presents a structure of a single-layered RLSA. Slots on the top plate consisting of many pairs, each one of which is a unit radiator of circular polarization, is arrayed spirally with the spacing $S\rho$ equal to the guide-wavelength λ_g. They are excited by a radially outward traveling wave in principle.

It is difficult to analyze more than a thousand slot pairs as it is. In practical design, we have analyzed the slot coupling in a linear array model on the rectangular waveguide with the periodic boundary conditions on its narrow walls [6] as is shown in Fig. 2(c) by assuming the rotational symmetry of the field. However, this model does not express spiral arrangement of slots rigorously. It also neglects the curvature of incidence wave which become notable in the central part of the aperture. Rotational symmetry of fields can only be discussed by analyzing the actual slot arrangement model in Fig. 2(b). We analyze the slot coupling in the first few turns of spiral cut on infinite parallel plates for a cylindrical traveling wave excitation. The upper and lower plates lie on the position $z=d$, 0, respectively. The power is fed at $(x, y)=(0, 0)$.

2. 2 Basis Function

The method of moment is applied to determine the aperture field of the slots. To derive a set of integral equations, the field equivalence theorem is applied. Every slot is replaced by an unknown equivalent magnetic current sheet backed with a perfectly conducting wall. The analysis model is then divided into two regions; the waveguide region (region 1) and the upper half space (region 2). For respective regions, the dyadic Green's functions $\boldsymbol{G}_{in}$ and $\boldsymbol{G}_{out}$ for the magnetic field produced by a unit magnetic current is derived. The continuity condition for the tangential magnetic fields on the j-th slot aperture S_j requires the integral relation as below:

$$\sum_i \iint_{S_i} \boldsymbol{G}_{out}(\boldsymbol{r}_j|\boldsymbol{r}_i)\,(\boldsymbol{E}_i \times \hat{\boldsymbol{z}})\,dS_i = \boldsymbol{H}_{in}(\boldsymbol{r}_j) + \sum_i \iint_{S_i} \boldsymbol{G}_{in}(\boldsymbol{r}_j|\boldsymbol{r}_i)\{\boldsymbol{E}_i \times (-\hat{\boldsymbol{z}})\}dS_i \quad (1)$$

where $\boldsymbol{E}_i$, $\hat{\boldsymbol{z}}$ and $\boldsymbol{H}_{in}$ are unknown electric field on the i-th slot, a unit vector in the z direction and the incident magnetic field, respectively.

For the reduction of Eq. (1) to a system of linear equations, Galerkin's method of moments is adopted. Firstly, the functional form of the unknown electric field $\boldsymbol{E}_i$ is assumed in the ith slot. A slot width is narrow in comparison with its length; the aperture electric field $\boldsymbol{E}_i$ is assumed to be purely polarized along the slot width. It is expressed in terms of unknown slot excitation coefficient v_i as

$$\boldsymbol{E}_i = v_i f(\xi_i)\, g(\eta_i)\, \hat{\eta} = v_i \boldsymbol{e}_i \quad (2)$$

where ξ_i and η_i are the local co-ordinates on the i-th slot, in the length and the width direction, respectively. The functions $f(\xi_i)$ and $g(\eta_i)$ are defined as

$$f(\xi_i) = \frac{\sin\{k_0(l_i/2 - |\xi_i|)\}}{\sin(k_0 l_i/2)} \quad (3)$$

$$g(\eta_i) = \frac{1}{\sqrt{(w/2)^2 - \eta_i^2}} \quad (4)$$

where l_i and w are the slot length of i-th slot and the slot width (common for all the slots), k_0 is the wavenumber in free space.

2. 3 Dyadic Green's Function

The external region is readily calculated in the spatial domain. The free space dyadic function in region 2 is given as [6]

$$\boldsymbol{G}_{out}(\boldsymbol{r}|\boldsymbol{r}_0) = -j\omega\varepsilon_0\left(\boldsymbol{I}+\frac{\nabla\nabla}{k_0^2}\right)\frac{\exp(-jk_0|\boldsymbol{r}-\boldsymbol{r}_0|)}{4\pi|\boldsymbol{r}-\boldsymbol{r}_0|} \quad (5)$$

where ω is the angular frequency, ε_0 is the permittivity of free space. The vectors' $\boldsymbol{r}$ and $\boldsymbol{r}_0$ denote the observation point and the source point, respectively. $\boldsymbol{I}$ is the unit dyadic. The operator ∇ indicates differentiation with respect to $\boldsymbol{r}$.

On the other hand, the dyadic Green's function for the fields inside the waveguide is calculated in spectral domain including all multimodes. The Fourier transformation is defined as

$$\tilde{\phi}(k_x, k_y) = \iint_{-\infty}^{\infty}\phi(x, y)\, e^{j(k_x x+k_y y)}dxdy \quad (6)$$

The dyadic Green's functions for the waveguide region satisfying the boundary conditions at $z=0$ and d are easily obtained as follows [10],[11];

$$\tilde{\boldsymbol{G}}_{in_{xx}}(k_x, k_y) = j\frac{\omega\varepsilon_1}{k_{1z}}\frac{k_1^2-k_x^2}{k_1^2}\cot(k_{1z}d) \quad (7)$$

$$\tilde{\boldsymbol{G}}_{in_{yx}}(k_x, k_y) = -j\frac{\omega\varepsilon_1}{k_{1z}}\frac{k_x k_y}{k_1^2}\cot(k_{1z}d) \quad (8)$$

$$k_1=\varepsilon_1 k_0;\ k_{1z}^2=k_1^2-k_x^2-k_y^2 \quad (9)$$

where ε_1, k_1 and d is the permittivity, the wavenumber in region 1 and waveguide height, respectively.

2. 4 Integral Equation

The integral equation (1) is multiplied by the basis function of the jth slot $\boldsymbol{e}_j\times\hat{\boldsymbol{z}}=\boldsymbol{M}_j$ and is integrated over the slot aperture. A set of linear equations for the unknown excitation coefficient v_j is given as [12]

$$\sum_{j=1}^{N} Y_{ij}v_j = I_i \quad (i=1, 2, \cdots, N) \quad (10)$$

where Y_{ij} is expressed as follows;

$$Y_{ij} = Y_{in_{ij}} + Y_{out_{ij}} \quad (11)$$

The external aperture admittance Y_{out} and the internal one Y_{in} are calculated in the spatial domain and the spectral domain, respectively; Y_{in} is expressed in term of the spectrum by using Parseval's theorem.

$$Y_{in_{ij}} = -\frac{1}{4\pi^2}\iint_{-\infty}^{+\infty}\tilde{\boldsymbol{M}}_i^*\cdot\tilde{\boldsymbol{G}}_{in}\cdot\tilde{\boldsymbol{M}}_j dk_x dk_y \quad (12)$$

where* denotes the complex conjugate. On the other hand Y_{out} and I_i are calculated in spatial domain as [13],[14]

$$Y_{out_{ij}} = \iint_{S_j}\iint_{S_i}\boldsymbol{M}_j\cdot\boldsymbol{G}_{out}\cdot\boldsymbol{M}_i dS_i dS_j \quad (13)$$

$$I_i = \iint_{S_i}\boldsymbol{H}_{in_i}\cdot\boldsymbol{M}_i dS_i \quad (14)$$

where $\boldsymbol{H}_{in}$ is the cylindrical incident magnetic field. The integrals in both sides of Eqs. (12) (13) contain only known functions $\tilde{\boldsymbol{G}}_{in}$, $\boldsymbol{G}_{out}$, and then the excitation coefficients of all the slots $v_j(j=1, 2, \cdots, n)$ are determined in Eq. (10).

2. 5 Inner Field

The inner field $\boldsymbol{H}(\boldsymbol{r})$ in the radial waveguide is the sum of the incident field and the scattering field from slots in Eq. (15).

$$\boldsymbol{H}(\boldsymbol{r}) = \boldsymbol{H}_{in}(\boldsymbol{r}) + \sum_{i=1}^{N}\boldsymbol{H}_{scat}(\boldsymbol{r}|\boldsymbol{r}_i) \quad (15)$$

where $\boldsymbol{H}_{scat}$ is the scattering field from slot as follows.

$$\boldsymbol{H}_{scat}(\boldsymbol{r}|\boldsymbol{r}_i) = v_i\int\boldsymbol{G}_{in}(\boldsymbol{r}|\boldsymbol{r}_i)\,\boldsymbol{M}_i dS_i \quad (16)$$

3. Numerical Results

The first few turns of slot pairs seem to disturb the inner field seriously. We calculated the inner field distribution in radial waveguide. Slot arrangement parameters of analysis model are listed in Table 1. To see the slot perturbations clearly, excessively coupled slots (number 1, 2) are analyzed first. The slot length ($\approx$8 mm) for the first turn in actual antennas is much smaller than this slot length ($\approx$11 mm). The measurement system is shown in Fig. 3. The probe (0.1λ monopole antenna) receives the power leaking from the annular slit in the aperture edge at $\rho=12$ cm. The waveguide end with slit is designed by using BEM (Boundary element method) [15], so that the reflection of less than -20 dB may be realized. The z component of the electric field is measured for the cylindrical outward traveling wave. If the wave is seriously

Table 1 Parameters of analysis models.

Slot Position ρ(cm)	Slot Length (mm)	Slot Number	Arrangement	Figure Number
4.2	11.3	2	------	Fig. 5
3.6~5.3	7.8,11.3	48	Spiral	Fig. 6
3.6~5.3 3.6~7.2	7.8~8.3 7.8~8.7	4,10,48 112	Spiral	Fig. 7
1.5~3.2	11.3	26	Spiral	Fig. 10(a)
3.5~5.2	11.3	46	Spiral	Fig. 10(b)
5.6~7.3	11.3	68	Spiral	Fig. 10(c)
4.2	11.3	44	Concentric	Fig. 11

Waveguide height d=3mm; Permittivity ε_1=1.53
Frequency 12.0GHz; Observing point ρ=12cm

perturbed from the cylindrical one, reflection and measurement error may increase. The unwanted reflection from the structure is further removed by using time gating technique of the network analyzer HP-8510C. Inner field of a radial line without slots is measured first to evaluate the errors in experiment. The measured amplitude and the phase are plotted in Fig. 4. The errors for cylindrical wave are less than about 0.5 dB in amplitude and 10 deg in phase.

Figure 5 shows the calculated inner field distribution for one slot pair. The inner field just behind slot pairs ($\phi \approx 0°$) is weak since the power is radiated from slots. On the other hand, the field becomes strong in angular regions on both sides of slot pairs ($\phi \approx 40°$, 320°), these angles correspond to main radiation direction of slots. Experimental results are also plotted by ○ in Fig. 5. The calculated values reasonably agree with theoretical one though the ripples in amplitude are a bit erroneous. These are the results for very strongly coupled slots and the inner field is seriously perturbed from the cylindrical wave. As is stated before, the measurement system in Fig. 3 is not so reliable. Figure 6 shows the predicted inner field distribution for 24 pairs array, where relatively shorter slots are used and the spacings between the adjacent pair is about 0.8 wavelength. These parameters are practically adopted in the commercialized model. Experimental results are also plotted by ○, showing good agreement with calculations. The predicted results for excessively coupling slots are also included in the figure for comparison. The rotational symmetry for weakly coupling slots is slightly better than that for strongly coupling ones but the perturbation of about 1dB and 20° still exists. Hereafter, we discuss strongly coupled slots for the application to prospective smaller aperture antennas.

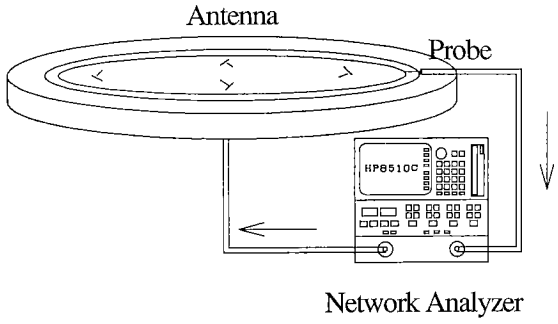

Fig. 3 Measurement system.

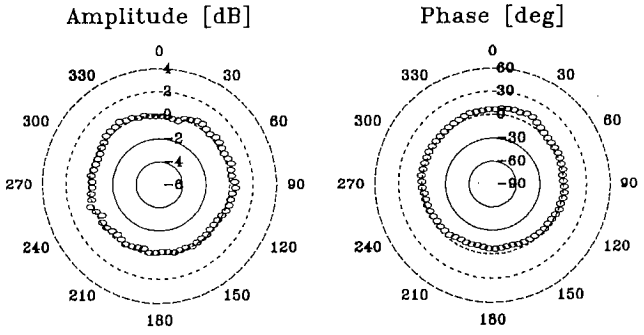

Fig. 4 Inner field distribution (no slots).
waveguide height $d=3$ mm; permittivity $\varepsilon_1=1.53$.
frequency 12.0 GHz; observing point $\rho=12$ cm.

In order to explain that the inner field disturbance is caused by the innermost slot pair in the spiral arrangement, Fig. 7 compares the field distributions for various number of slot pairs in two turns spiral arrangement; they are the innermost (A) two ($0°<\phi<35°$) and (B) five ($0°<\phi<90°$) slot pairs, (C) slot pairs on the first turn and (D) those on the two turns. The first pair is at $\phi=0°$ in all cases. In the angular region 300~330°, the two ripples appear in every case and indicate the influence of the innermost slot pair. It is understood that once the field is disturbed by the first pair, it propagates radially outward as it is, and the location of ripples is not changed. This fact indicates that the influence of the innermost slot pair dominates the illumination disturbance (in Fig. 1).

To extract the necessary condition for suppressing the higher mode with ϕ variation, we may focus upon the annularly arrayed pairs as in Fig. 8 instead of actual spiral array (Fig. 2(b)). The number of slot

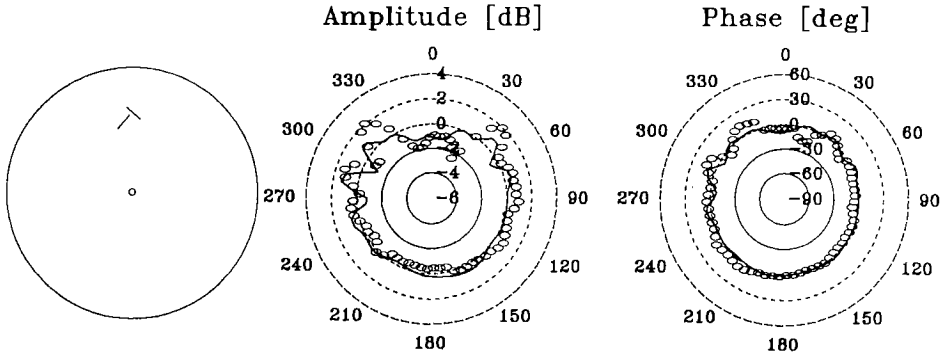

Fig. 5 Inner field distribution (1 slot pair).
○: Exp. ——: Cal.

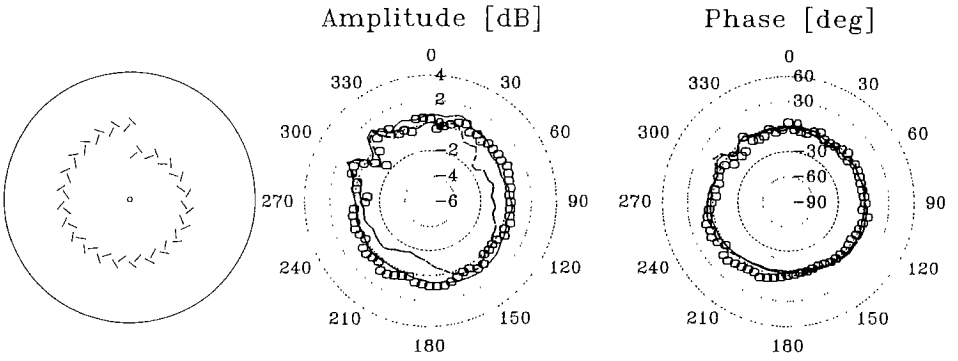

Fig. 6 Inner field distribution as a various slot coupling.
(a) Strong coupling: slot length=11.3 mm------.
(b) Actual coupling: slot length=7.8 mm——.
○: Exp.

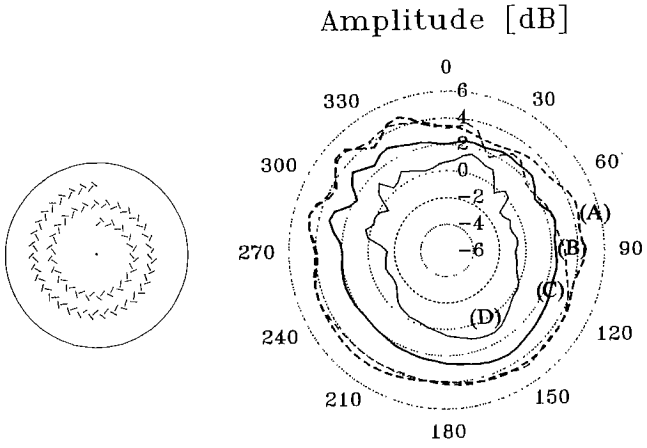

Fig. 7 Influence of the innermost slot pair.

----- 2slot pairs (A)
----- 5 slot pairs (B)
—— 1 turn (24 slot pairs) (C)
—— 2 turns (56 slot pairs) (D)

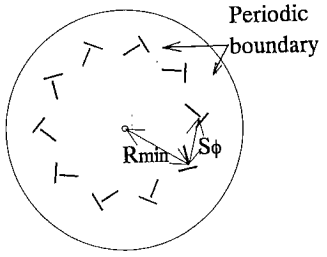

Fig. 8 Definition of S_ϕ and $R_{\min}$. (Annular model).

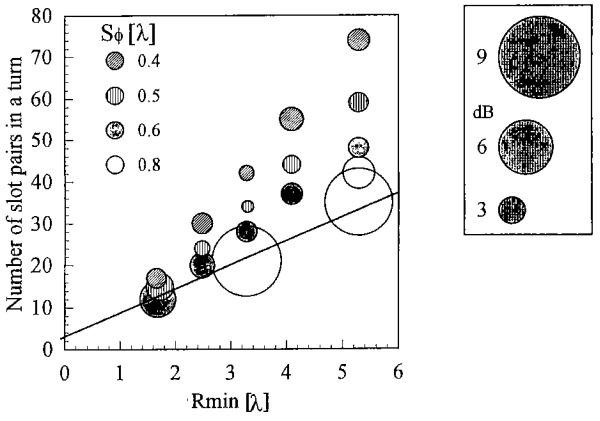

Fig. 9 Disturbance of the iner field for the actual array.
$\varepsilon_r=1.53$.
——Cutoff mode number: $\sqrt{\varepsilon_r}2\pi R_{\min}$ from Eq. (17).

pairs in a turn is m; the lowest higher mode in Fig. 8 has the mode number m. $R_{\min}$ is the radial location of the innermost slot pairs and S_ϕ is the spacing in the angular direction. The cutoff wavelength in the radial waveguide is given in Eq. (17) [16].

$$\lambda_c=\frac{\lambda_{c0}}{\sqrt{\varepsilon_r}}=\frac{1}{\sqrt{\left(\frac{n}{2d}\right)^2+\left(\frac{m}{2\pi R_{\min}}\right)^2}}$$

$$=\frac{2\pi R_{\min}}{m}\cong S_\phi \quad (n=0) \tag{17}$$

where n is the mode number of the waveguide height direction and λ_{c0} is the cutoff wavelength in the free space. Since the waveguide height d is thin enough, $n=0$ is assumed. In order to maintain only the TEM mode, $\lambda>\sqrt{\varepsilon_r}\,S_\phi$ is necessary, where λ is the free space wavelength in operating frequency. This corresponds to the dominant mode condition for the conventional analysis model of rectangular waveguide with periodic boundary (Fig. 2(c)). This observation is valid only for annular array in Fig. 8 but is giving the necessary condition for the practical spiral array in Fig. 2(b) as well. To confirm the applicability of this condition to the spiral model, Fig. 9 shows the simulated disturbance of the inner field for the actual spiral array in Fig. 2(b) as a function of $R_{\min}$. The radius of a circle

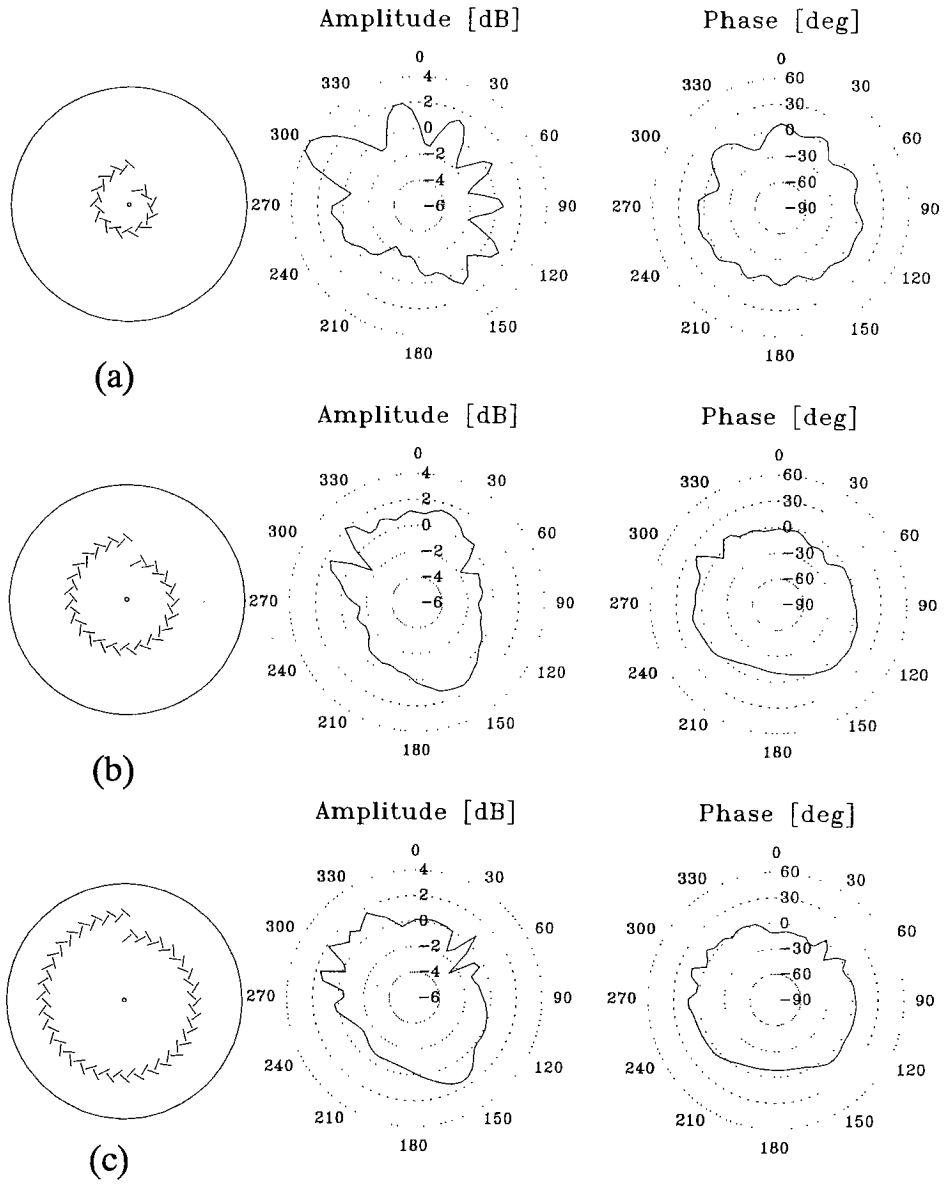

Fig. 10 Inner field distribution (various slot location) (S_ϕ=0.5λ).
(a) 13 slot pairs. (b) 23 slot pairs. (c) 34 slot pairs.

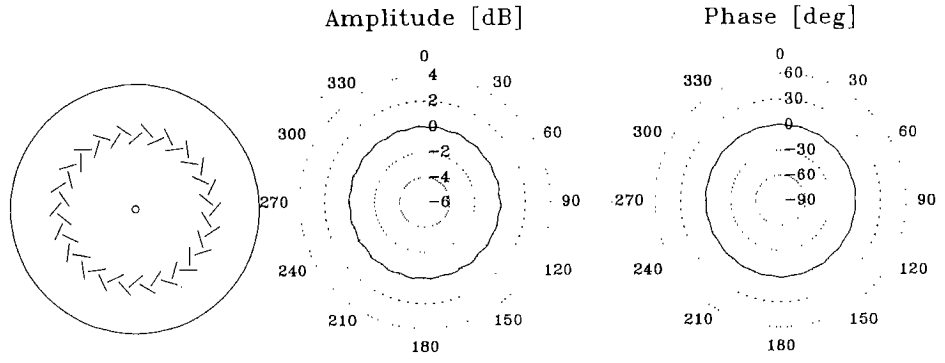

Fig. 11 Inner field distribution (22 slot pairs—Concentric—).

indicates the value of peak disturbance. When the number of slot pairs (m) is reduced to $\sqrt{\varepsilon_r}\frac{2\pi R_{\min}}{\lambda}$, the disturbance becomes large. This suggests the general design requirement that the slot pair spacings in the angular direction should be much smaller than the guide wavelength. This reflects the defect of the spiral arrangement in comparison with the annular arrangement.

One observation which is unique for spiral is discussed next. In Fig. 10, S_ϕ and the slot length remain unchanged in all the cases but only radial location of the innermost slot pairs ($R_{\min}$) is varied. The rotational symmetry is getting better as the location of innermost slot pair becomes outer. In the strict sense, $S_\phi<\lambda/\sqrt{\varepsilon_r}$ is only the necessary and is not the sufficient condition.

We have proposed concentric slot arrangement of RLSA excited by a rotating mode instead of rotationally symmetric mode [17]. In Fig. 11, slot pairs are concentrically arranged and are excited by a rotating mode $e^{j\phi}$ for $S_\phi=0.5\lambda$. The phase distribution for the rotation is subtracted from the results in the figure. Note that, in Fig. 11, ripples are smaller than the spiral arrangement in Fig. 10(b) with the same S_ϕ. In spiral arrangement, two ripples at $\phi\cong 300$, 330° indicate the effect of the innermost pairs. However, in concentric slot pair's arrangement (Fig. 11), the inner field distribution is almost uniform. The concentric slot arrangement of RLSA is very attractive for smaller RLSA where stronger slot coupling and higher efficiency is aimed. This will be used jointly with the matching element [9] at the terminal of the aperture to reduced the reflection and the loss power at the termination. The reflection of less than -20 dB has already been confirmed by experiments of 25 cm diameter model antenna, therefore the results derived assuming only the outward traveling wave is directly applicable for smaller antennas.

4. Conclusion

This paper presented the analysis of the inner field in radial waveguide. We calculate the perturbation of the inner field distribution due to the first few turns of spiral arrangement. The calculated results are verified by the experiments and fine agreement is demonstrated. The main reason of the inner field disturbance is highly dependent upon the slot pair arrangement and its coupling strength. Theoretical results show that the innermost pair has the most important affects. Excessive coupling may seriously disturb the symmetry. For enhancing the rotational symmetry, the slot pair should be located as far as possible from the center. In addition, slot pairs in the first turn are arranged as densely as possible. The inner field disturbance is drastically reduced when slot pairs are arranged concentric and a rotating mode excitation is adopted. The analysis for full array seems computationally impossible even in the future but the results obtained in this paper for smaller number of slots give fruitful information for the practical design of RLSAs.

Acknowledgment

Calculations were carried out on super computer ETA10 of computer center, Tokyo Institute of Technology.

References

[1] Goto, N. and Yamamoto, M., "Circularly polarized radial line slot antennas," *IECE Technical Report*, AP80-57, Aug. 1980.

[2] Ando, M., Sakurai, K., Goto, N., Arimura, K. and Ito, Y., "A radial line slot antenna for 12GHz satellite TV reception," *IEEE Trans. Antennas & Propag.*, vol. 33, no. 12, pp. 1347-1353, Dec. 1985.

[3] Takahashi, M., Takada, J., Ando, M. and Goto, N., "A slot design for uniform aperture field distribution in single-layered radial line slot antennas," *IEEE Trans. Antennas & Propag.*, vol. 39, no. 7, pp. 954-959, Jul. 1991.

[4] Takahashi, M., Takada, J., Ando, M. and Goto, N., "Characteristics of small-aperture single-layered radial line slot antennas," *IEE Proc. Pt. H*, vol. 139, no. 1, pp. 79-83, Feb. 1992.

[5] Takahashi, M., Takada, J., Ando, M. and Goto, N., "Aperture illumination control in radial line slot antennas," *IEICE Trans. Commun.*, vol. 76, no. 7, Jul. 1993.

[6] Hirokawa, J., Ando, M. and Goto, N., "An analysis of slot coupling in a radial line slot antenna for DBS reception," *IEE Proc. Pt. H*, vol. 137, no. 5, pp. 249-254, Oct. 1990.

[7] Takahashi, M., Ando, M. and Goto, N., "A rotational symmetry in single-layered radial line slot antennas," *Proc. of 1992 Autumn Conf.*, vol. B-74, Sep. 1992.

[8] Takahashi, M., Natori, M., Takada, J., Ando, M. and Goto, N., "A single-layered radial line slot antenna for DBS reception," *3rd Asia-Pacific Microwave Conf.*, 5-2, pp. 75-78, Sep. 1990.

[9] Ueno, M., Takahashi, M., Hirokawa, J., Ando, M., Goto, N. and Arai, H., "A rotating mode radial line slot antenna—concentric array—," *IEICE Technical Report*, AP-93-43, Jun. 1993.

[10] Nakamura, T. and Ito, K., "A basic study of integrated antennas," *IEICE Technical Report*, EMT-89-44, 1989.

[11] Itoh, T., ed., "Spectral domain approach," in *Basic analyses for electromagnetic wave problems*, ed. E. Yamashita, IEICE, 1987.

[12] Kominami, M., Takei, T. and Rokushima, K., "A print dipole electromagnetically coupled to a microstrip feed line," *Trans. IEICE*, vol. J70-B, no. 2, pp. 233-241, Feb. 1987.

[13] Richmond, J. H. and Geary, N. H., "Mutual impedance between coplanar-skew dipoles," *IEEE Trans. Antennas & Propag.*, vol. AP-18, pp. 414-416, May 1970.

[14] Seki, H., *Moment and variational analysis of slotted waveguide antennas and its applications*, Doctoral dissertation, Tokyo Inst. of Tech., Dec. 1981.

[15] Ueno, M., Takahashi, M., Hirokawa, J., Ando, M. and Goto, N., "Matching elements for radial line slot antennas," *Proc. IEICE Spring Conf. '93*, B-50.

[16] Marcuvitz, N., "Waveguide Handbook," *IEE Electromagnetic waves series 21*, Peter Peregrinus Ltd., pp. 89–96, 1986.

[17] Hosono, S., Hirokawa, J., Ando, M., Goto, N. and Arai, H., "Feeding circuit for radial-line waveguide using an electric wall type cavity resonator," *Proc. IEICE Fall Conf. '93*, B-56.

Masaharu Takahashi was born in Chiba, Japan, on December 15, 1965. He received the B.E. degree in electrical engineering in 1989 from Tohoku University, Miyagi, Japan, and the M.E. and D.E. degree in electrical engineering from Tokyo Institute of Technology, Tokyo, Japan, in 1991 and 1994, respectively. He is currently a Research Associate at Musashi Institute of Technology, Tokyo, Japan. His main interests have been electrically small antennas and planar array antennas.

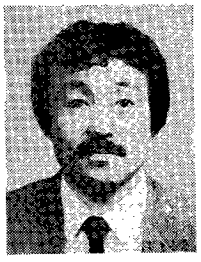

Makoto Ando was born in Hokkaido, Japan, on February 16, 1952. He received the B.S., M.S. and D.E. degrees in electrical engineering from Tokyo Institute of Technology, Tokyo, Japan in 1974, 1976 and 1979, respectively. From 1979 to 1983, he worked at Yokosuka Electrical Communication Laboratory, NTT, and was engaged in development of antennas for satellite communication. He was a Research Associate at Tokyo Institute of Technology from 1983 to 1985, and is currently an Associate Professor. His main interests have been high frequency diffraction theory such as Physical Optics and Geometrical Theory of Diffraction. His research also covers the design of reflector antennas and waveguide planar arrays for DBS and VSAT. He received the Young Engineers Award of IECE Japan in 1981, the Achievement Award and the Paper Award from IEICE Japan in 1993. He also received the 5th Telecom Systems Award in 1990 and the 8th Inoue Prize for Science in 1992.

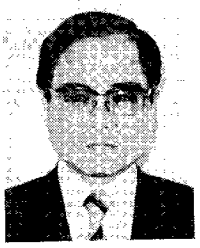

Naohisa Goto was born in Utsunomiya, Japan, on June 8, 1935. He received the B.S., M.S. and D.E. degrees from Tokyo Institute of Technology, Tokyo, Japan, all in electrical engineering, in 1959, 1961 and 1964, respectively. From 1966 to 1968 he was an Associate Professor at the Training Institute for Engineering Teachers, Tokyo Institute of Technology. From 1968 to 1975 he was an Associate Professor at Chiba University, Chiba, Japan. From 1975 to 1980 he was an Associate Professor, and since 1980 he has been a Professor at Tokyo Institute of Technology. He has been engaged in research and development of array antennas. He has developed a planar slotted waveguide array called "radial line slot antenna," and a ring patch antenna for dual frequency use called "self-diplexing antenna."